Assembly, translocation, and activation of XerCD-*dif* recombination by FtsK translocase analyzed in real-time by FRET and two-color tethered fluorophore motion

Peter F. J. May[a], Pawel Zawadzki[b], David J. Sherratt[b], Achillefs N. Kapanidis[a,1], and Lidia K. Arciszewska[b,1]

[a]Biological Physics Research Group, Clarendon Laboratory, Department of Physics, University of Oxford, Oxford OX1 3PU, United Kingdom; and [b]Department of Biochemistry, University of Oxford, Oxford OX1 3QU, United Kingdom

Edited by Stephen J. Benkovic, The Pennsylvania State University, University Park, PA, and approved July 31, 2015 (received for review June 2, 2015)

The FtsK dsDNA translocase functions in bacterial chromosome unlinking by activating XerCD-*dif* recombination in the replication terminus region. To analyze FtsK assembly and translocation, and the subsequent activation of XerCD-*dif* recombination, we extended the tethered fluorophore motion technique, using two spectrally distinct fluorophores to monitor two effective lengths along the same tethered DNA molecule. We observed that FtsK assembled stepwise on DNA into a single hexamer, and began translocation rapidly (~0.25 s). Without extruding DNA loops, single FtsK hexamers approached XerCD-*dif* and resided there for ~0.5 s irrespective of whether XerCD-*dif* was synapsed or unsynapsed. FtsK then dissociated, rather than reversing. Infrequently, FtsK activated XerCD-*dif* recombination when it encountered a preformed synaptic complex, and dissociated before the completion of recombination, consistent with each FtsK–XerCD-*dif* encounter activating only one round of recombination.

tethered fluorophore motion | DNA translocation | site-specific DNA recombination | chromosome segregation | single-molecule FRET

Understanding how molecular machines assemble and act requires a combination of biochemical, structural, and biophysical approaches. In recent years, single-molecule techniques have allowed the observation of biological reactions in real time, thereby avoiding the averaging of ensemble experiments. These single-molecule studies rely on information gained from existing biochemical characterization to set experimental parameters and to place their results in context. To follow complex multistep reactions involving multiple components, methods capable of tracking several observables simultaneously have been established (1–4). In this work, we push the boundaries of a recently developed technique, and apply it to further our understanding of the *Escherichia coli* XerCD-*dif*–FtsK molecular machine, which functions in chromosome segregation and coordinates it with cell division.

FtsK is a 1,329-aa DNA translocase, which assembles at the division septum and functions in segregating sister chromosomes during the late stages of the cell cycle in a wide range of bacteria (5–8) by activating site-specific recombination by XerCD at *dif* (9). The two related Tyr recombinases, XerC and XerD, bind the 28-bp *dif* site located within the terminus region, *ter*, on the *E. coli* chromosome. They unlink catenated chromosomes and resolve chromosome dimers formed by homologous recombination (10–14). Independent of its role in activating XerCD-*dif* recombination, FtsK appears to play a direct role in the segregation of *ter* (8). FtsK consists of three domains: an essential 179-aa N-terminal domain that anchors it to the division septum, an ~500-aa C-terminal motor domain, and an ~650-aa linker domain (6, 7, 15, 16). The motor domain, $FtsK_C$, is composed of α-, β-, and γ-subdomains (17). The α- and β-subdomains form a dsDNA translocase, belonging to the RecA family of ATPases (17). The γ-subdomain plays a regulatory role in the recognition of the FtsK orientating polar sequence (KOPS) that guides FtsK translocation toward the *dif* site at *ter* (18–20), and in the activation of XerCD-*dif* recombination (9, 14, 21). Activation of recombination requires direct interaction between the γ-subdomain and XerD (22, 23).

Our previous work, using a single tethered fluorophore motion (TFM) reporter, in combination with Förster resonance energy transfer (FRET), determined the conformational transitions in the XerCD-*dif* complex that occurred as XerD mediated an initial strand exchange to form a Holliday junction (HJ), which was resolved by a subsequent XerC-mediated strand exchange (24). In that work, we indirectly inferred the presence of $FtsK_C$, taking advantage of protein-induced fluorescence enhancement (PIFE) (25). Here, we have expanded TFM-FRET, using two spectrally distinct TFM reporters (one on $FtsK_C$ and one on DNA), to directly observe $FtsK_C$ as it assembles and translocates, and to correlate its behavior, upon arrival at XerCD, with the progress of the recombination reaction.

Previous studies of $FtsK_C$ assembly and translocation have used biochemical methods (26, 27) and single-molecule techniques, including magnetic and optical tweezers (18, 28–30); tethered particle motion (TPM) (18); and, more recently, DNA curtains (31, 32). Optical/magnetic tweezers and TPM experiments have relied on loop extrusion by $FtsK_C$ to observe its action (looping by FtsK shortens the length between two DNA ends, hence displacing the bead used in TPM or optical/magnetic tweezers). Many of the single-molecule assays involved the attachment of $FtsK_C$ to quantum dot (QD) labels or used derivatives

Significance

This study develops and exploits an expanded single-molecule fluorescence technique to understand the molecular mechanism of assembly, translocation, and disassembly of a hexameric DNA motor, FtsK, which functions ubiquitously in bacterial chromosome segregation. Assembly of single hexamers on DNA and their subsequent rapid translocation were directly assayed. FtsK hexamers dissociated soon after encountering and activating XerCD-*dif* recombination complexes. This work contrasts with previously published reports, which suggested that FtsK can reverse spontaneously during translocation, or upon encountering XerCD-*dif*. Furthermore, in some previous assays, the readout was DNA looping; here, we show that looping does not occur with single hexamer translocation. The technique used provides a blueprint for mechanistic real-time studies of individual protein–nucleic acid complexes.

Author contributions: P.F.J.M., D.J.S., A.N.K., and L.K.A. designed research; P.F.J.M. performed research; P.F.J.M. contributed new analytic tools; P.F.J.M. and P.Z. contributed new reagents; P.F.J.M. analyzed data; and P.F.J.M., D.J.S., A.N.K., and L.K.A. wrote the paper.

The authors declare no conflict of interest.

This article is a PNAS Direct Submission.

Freely available online through the PNAS open access option.

[1]To whom correspondence may be addressed. Email: a.kapanidis1@physics.ox.ac.uk or lidia.arciszewska@bioch.ox.ac.uk.

This article contains supporting information online at www.pnas.org/lookup/suppl/doi:10.1073/pnas.1510814112/-/DCSupplemental.

that were known to aggregate, thereby potentially confounding the interpretation of data, because multiple motors could be present in the region of analysis. Experiments utilizing DNA curtains have revealed that $FtsK_C$ can push, evict, and bypass proteins bound to DNA as it translocates (32). However, $FtsK_C$ stops at least transiently and/or dissociates at XerCD bound to *dif* (27, 32). Reversals in translocation direction have been observed to occur spontaneously (18, 28, 30, 31) and in response to XerCD bound to *dif* (32). The use of a fluorophore label, along with singly tethered DNA, has allowed us to observe $FtsK_C$ without requiring any loop extrusion, and to observe its interaction with synaptic complexes of XerCD, where previous single-molecule work has only dealt with unsynapsed XerCD-*dif* (32). Using this approach, we have determined that $FtsK_C$ assembles on DNA as a single hexamer, and begins translocating rapidly (~0.25 s), without extruding a loop of DNA. When it reached XerCD bound to *dif*, either in a synapsed or unsynapsed conformation, it resided briefly for ~0.5 s and then dissociated without any evidence of reversal. $FtsK_C$ activated recombination when it met synapsed XerCD-*dif* complexes, and then dissociated faster than the completion of recombination by XerCD.

Results

Spectrally Separate Fluorophores Report on DNA Conformation and $FtsK_C$ Behavior. We adapted TFM-FRET (24, 33, 34) to follow the assembly, translocation, and behavior of $FtsK_C$ when it interacts with XerCD. We made a DNA substrate carrying two *dif* sites separated by a 1-kb spacer (Fig. 1*A*). The substrate was attached to the slide surface through a biotinylated 5′ end that was located 200 bp away from the first surface-proximal *dif* site, and the second surface-distal *dif* site was flanked by a 2.8-kb DNA segment containing a triple KOPS near its end. The KOPS was orientated toward the surface (Fig. 1*A*, Fig. S1*A*, and *Methods*). The DNA was labeled with Cy3B 1 bp away, in the direction of the free end, from the XerD binding sequence of the surface-distal *dif* site. TFM uses the width of the image of this single fluorophore to measure an effective distance along DNA; the fluorescence image width (FIW) decreases as the effective tether length decreases. Synapsis formation between the two *dif* sites, mediated by XerCD, was evident as a reduction in the green (Cy3B) FIW, and recombination was evident as a permanent reduction in the green FIW (Fig. 1*A*).

We used a covalent trimer of $FtsK_C$ (35), singly labeled with Cy5 at a surface Cys introduced in the motor β-subdomain of the middle monomer (Cy5-FtsK, with a labeling efficiency of ~50%; Fig. S1 *B–F* and *Methods*). The trimer concentration, 5 nM, was close to the ~40 nM in vivo monomer concentration (36). The binding of $FtsK_C$ was apparent as an appearance of signal in the red (Cy5) channel, and the position and behavior of the $FtsK_C$ were monitored via the red FIW (Fig. 1*B*). To convert between the red FIW and the position of $FtsK_C$ along DNA, we imaged dsDNA, with lengths between 87 and 4,000 bp, using our total internal reflection fluorescence (TIRF) microscope and standard conditions of 25-ms alternating laser excitation (ALEX) (37) (Fig. 1*C* and *Methods*). At around a 1-kb tether length, with the 400 photons per 25-ms frame observed using our illumination power (corresponding to a 16-kHz emission rate), we would need to measure for 15 frames (~400 ms of observation time) to be able to distinguish with 95% confidence a 500-bp difference in effective tether length (Fig. 1*C*). The spatial and temporal resolution of TFM is discussed in our previous work (34).

In the absence of ATP and XerCD, we observed transient binding events that showed no obvious translocation (Fig. S2*A*); these binding events were distributed randomly along the DNA (Fig. S2*B*). The $FtsK_C$ dwell time was fit using three exponentials (Fig. S2*C* and *Methods*), recovering a major time of 0.84 ± 0.07 s (61 ± 5%) and two minor times of 4.0 ± 0.9 s (18 ± 5%) and 24 ± 3 s (19 ± 3%). We attribute the shortest time to transient

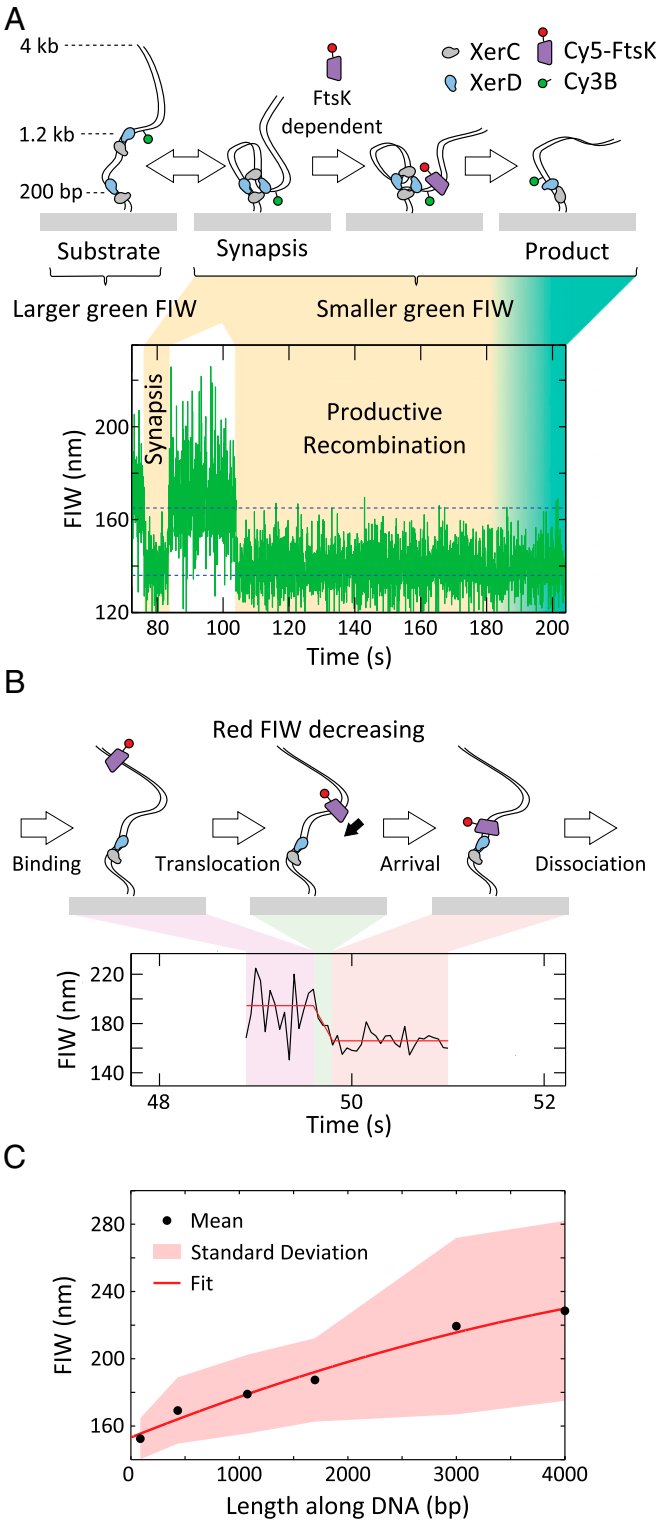

Fig. 1. Experimental design. (*A*) Recombination is monitored using Cy3B. Synapsis transiently reduces the fluorescence image width (FIW), and recombination permanently reduces FIW. Blue dashed lines represent population average FIWs for the unsynapsed and synapsed/product DNA (165 nm and 136 nm, respectively). (*B*) Cy5 monitors $FtsK_C$ behavior. Translocation decreases or increases FIW. The red line represents LS fit, which was used to segment translocation. (*C*) FIW calibration. The SD from frame to frame over all of the molecules is shown as the shaded region. The red line represents a quadratic LS fit ($n > 50$ at each DNA length).

association of a single Cy5-FtsK with DNA, the intermediate time to formation of a hexamer from two Cy5-FtsK molecules on DNA (because a hexamer would be more stable than a trimer), and the longest time to nonspecific sticking to the surface of the slide and subsequent photobleaching (photobleaching time for Cy5 at the surface was 28 ± 3 s) (Fig. S1*D*). These nonspecific sticking events were distinguished by their fixed narrow red FIW and were excluded from further analysis. Hence, around a quarter of DNA binding events had a dwell time that indicated hexamer assembly.

In the presence of ATP, in addition to transient binding events (Fig. S3*A*), we observed events with a decreasing red FIW, consistent with Cy5-FtsK translocations along DNA (Fig. 2*A* and Fig. S3*B*). We used a least-squares (LS) fit to the red FIW (*Methods*) to segment translocation events into three stages: assembly before translocation, translocation, and residence after translocation. The mean FIW before translocation, 220 nm, corresponded to the position of the KOPSs (FIW ≈ 230 nm), and the mean FIW after translocation, 161 nm, corresponded to close to the surface (FIW ≈ 155 nm), past the Cy3B (FIW ≈ 183 nm) (Figs. 1*C* and 2*B*), indicating that Cy3B does not impede $FtsK_C$ translocation. These mean FIWs suggest that the translocating $FtsK_C$ we observe assembles at or near the KOPSs and translocates past Cy3B, reaching the surface attachment point of the DNA. FRET, which reports the proximity of Cy5-FtsK to Cy3B within ~10 nm [Förster radius, R_0 ≈ 6.5 nm for these fluorophores (24)], was not observed under these conditions. Occasionally (n = 7), the red and green fluorescence disappeared simultaneously, which indicated that $FtsK_C$ had displaced the biotin–neutravidin interaction that tethered the DNA to the surface (Fig. S3*C*). This rare displacement is consistent with previously described behavior (38).

We determined the duration of $FtsK_C$ assembly, translocation, and residence using the LS fit to the red FIW. We found that dwell time distributions were in better agreement with two independent exponential processes rather than one, as judged using the Bayesian information criterion (BIC) (39) (ΔBIC > 10 in all

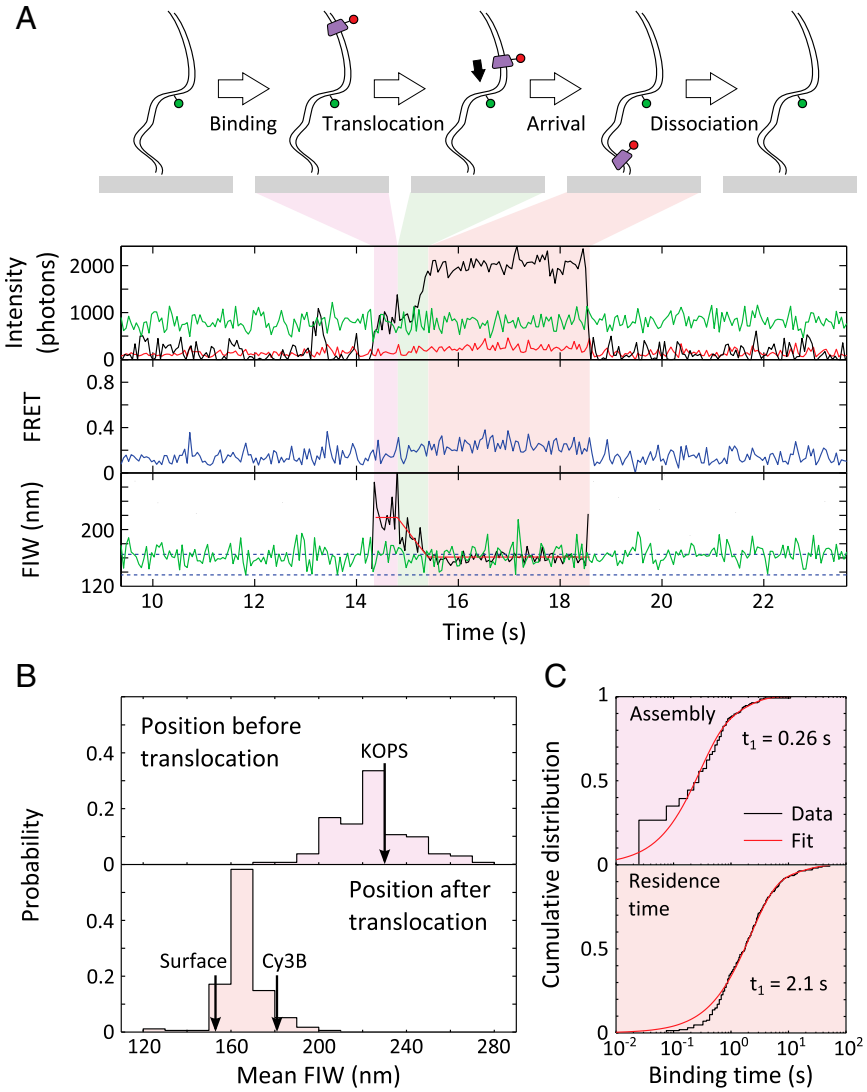

Fig. 2. Translocation events in the absence of XerCD. (*A*) Translocation event. (*Top*) Intensity: green emission under green excitation (*DD*, green), red emission under green excitation (*DA*, red), and red emission under red excitation (*AA*, black). (*Middle*) Apparent FRET. Under these conditions, no FRET was observed. (*Bottom*) FIW in the green channel (green) and in the red channel (black), and LS fit to the red FIW (red) used to segment the event into before (purple shading), during (green shading), and after (orange shading) translocation (n = 179 events). (*B*) Start and end positions of translocations. Black arrows represent positions of features on the DNA, obtained using the FIW calibration. (*C*) Dwell times. (*Top*) $FtsK_C$ assembly. (*Bottom*) Residence after translocation. Distributions were fit using a two-exponential process (Table S1 and *Methods*).

cases, indicating strong evidence in favor of a two-exponential model). Hence, except where otherwise noted, we fit dwell time distributions with two exponentials and restrict our discussion to the major population (Table S1). Averaging across all fits to dwell times, the major population accounts for ∼90% of dwells, and we suggest that the minor population is a fit to background events. Using this method, the assembly time before translocation was 0.26 ± 0.12 s and the residence time after translocation was 2.1 ± 0.2 s (Fig. 2*C*, Table S1, and *Methods*). The mean translocation time was 0.33 ± 0.02 (±SEM), which corresponds to a translocation velocity of 12 ± 1 kb·s^{-1} at 21 °C (given that translocation events originated at the KOPS and ended close to the surface), which is a factor of two faster than previously measured at this temperature (30), but we note that our method did not require looping by FtsK$_C$ or the movement of a large bead with associated hydrodynamic drag to observe translocation. Hence, this velocity corresponds to the physiological translocation speed along unconstrained, flexible, "naked" dsDNA.

A minority of events (n = 8, compared with 176 obvious translocations) showed a decrease in the green FIW, during the time that FtsK$_C$ was bound to DNA, which could be interpreted as the sticking of FtsK$_C$ to the surface or translocation-induced looping (Fig. S3*D*). These results establish that, in general, translocation does not induce DNA looping.

Stoichiometry of Translocating FtsK$_C$. Previous biochemical analysis has suggested that the translocating unit of FtsK$_C$ assembles on DNA in six steps to form single hexamers (26). However, double-ring structures that could correspond to head-to-head hexamers on DNA have been observed in electron micrographs of *Pseudomonas aeruginosa* FtsK$_C$ lacking the γ-subdomain, and crystal structures of this protein contained dodecameric ring structures (17). To assess the stoichiometry of the active unit of FtsK$_C$ directly, we measured the intensities of Cy5-FtsK and counted the number of fluorophores present during assembly and during interactions with XerCD. A single hexamer, made up of two labeled trimers, would have between one and two fluorophores attached, and a double hexamer would have between one and four fluorophores attached.

For this analysis, we used the shorter, single *dif*-containing, DNA fragments formed by XerCD recombination at the surface (Fig. S4*A*), because all features of the DNA (*dif* site, KOPS, and Cy3B) were 1,000 bp closer to the surface than in the original substrate, and hence in a region of higher illumination intensity in the evanescent field of TIRF. This DNA recombinant product was identified as having a permanent narrow green FIW. Translocation events were segmented as before (Fig. S4*B*). If FtsK$_C$ preassembled in solution and then bound DNA fully assembled, we would predict no change in intensity between FtsK$_C$ binding and the start of translocation; however, if FtsK$_C$ assembled on DNA, the intensity should increase before translocation begins (Fig. 3*A*). The mean intensities during assembly, across all translocation events, were extracted (Fig. 3*B*). At a time 0.5 s after the appearance of red fluorescence signaling the presence of FtsK$_C$, more than 66% of translocations had begun (Fig. S4*C*). We saw that on this time scale, there was a clear increase in the intensity of the red signal without any change in FIW (Fig. 3*B*), which implies that there was a stepwise assembly of Cy5-FtsK before translocation. Given our labeling efficiency of ∼50%, if FtsK$_C$ assembled into a single hexamer composed of two trimers, we would anticipate an average increase of 33%, and if it assembled into a double hexamer, we would anticipate an average increase of 110% before translocation (*Methods*). The observed 38.5% increase in intensity during the 0.5 s after binding is consistent with assembly into a single hexamer (Fig. 3*B*). The intensity increase suggests that FtsK$_C$ assembles on DNA rather than in solution. Using biotinylated anti-His antibodies, we pulled Cy5-FtsK out of solution, and determined that, at 5 nM and in the absence of DNA,

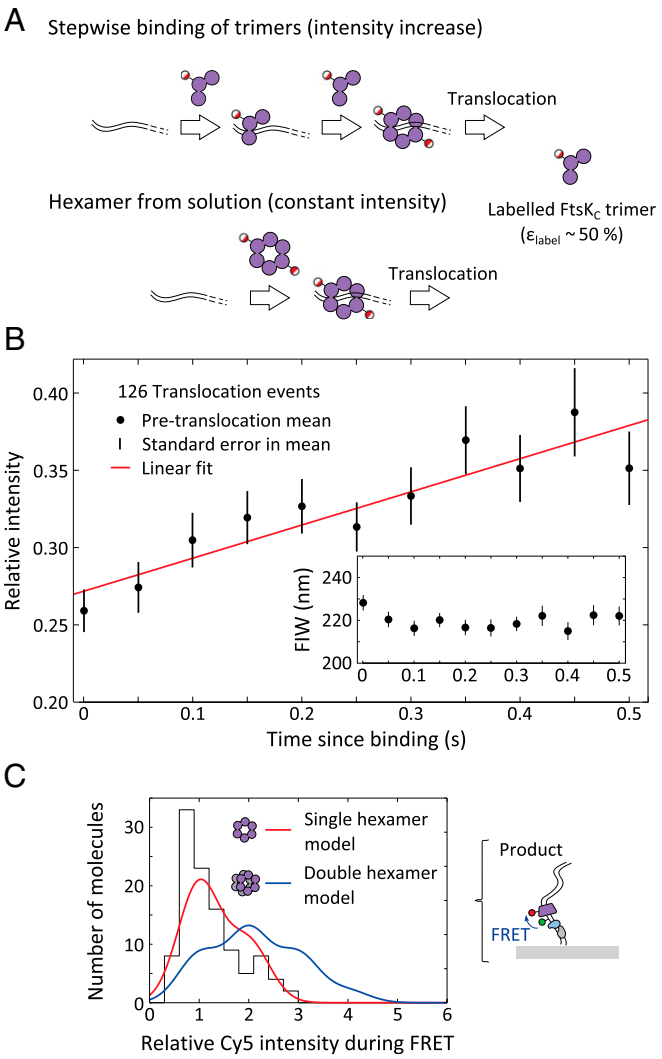

Fig. 3. FtsK$_C$ stoichiometry. (*A*) Intensity changes before translocation. If FtsK$_C$ assembles in a stepwise fashion before translocation, we expect an increase in intensity before translocation starts, whereas if fully assembled oligomers in solution bind and translocate, there would be no increase. (*B*) Mean relative intensity before translocation. A single Cy5 had a relative intensity of 0.2–0.4 between 2 and 3 kb along the DNA (*Methods*). Error bars: ±SEM. Least-squares fit (red) with an intensity increase of 38.5 ± 0.2% in the 0.5 s since binding (by which time more than 66% of translocations have begun). (*Inset*) Mean FIW for the same molecules. (*C*) Cy5 intensity during FRET. (*Right*) Corrected intensity during FRET events for the product DNA conformation were extracted and histogrammed (n = 108). (*Left*) Predicted intensity distribution is shown for a single hexamer (red) and a double hexamer (blue) of FtsK$_C$. A single hexamer provides a better explanation of our data [single hexamer: sum of squared deviation (SSD) = 330; double hexamer: SSD = 1,230].

the predominant stoichiometry was a single trimer (Fig. S1*F*), consistent with stepwise assembly on DNA before translocation.

We also determined the stoichiometry of FtsK$_C$ during its interaction with XerCD complexes. In the presence of Cy5-FtsK, ATP, and XerCD, we observed FRET, signaling proximity between Cy5-FtsK and the Cy3B placed near the XerD binding site (Fig. S4*A*). We used the Cy5 intensity during FRET to extract the number of Cy5 fluorophores attached to a FtsK$_C$ complex while it interacted with XerCD-*dif* (*Methods*). This intensity was expressed relative to the calculated intensity for a single Cy5 at the same position (40) (*Methods*). Using this intensity for a single fluorophore, the labeling efficiency of Cy5-FtsK, and the width

of the intensity distribution for a single fluorophore (Fig. S1*E*), we predicted the intensity distribution for a single hexamer and a double hexamer (Fig. 3*C*, Fig. S5, and *Methods*). Across all DNA conformations, the data agree much better with the single-hexamer prediction (Fig. 3*C* and Fig. S5). Hence, we conclude that, consistent with its assembly into a single hexamer before translocation, $FtsK_C$ interacts with XerCD as a single hexamer.

Interactions Between Translocating $FtsK_C$ and XerCD-*dif* Complexes. FtsK activates site-specific recombination by XerCD, and biochemical studies have shown that when $FtsK_C$ encounters XerD during translocation, it stops there (27). Moreover, QD-labeled $FtsK_C$ has been observed to pause and reverse translocation direction after meeting unsynapsed XerCD-*dif* on DNA curtains (32). In this work, we use singly Cy5-labeled $FtsK_C$ and observe its interaction with XerCD-*dif* in both unsynapsed and synapsed configurations.

We imaged our double-*dif* tethered DNA substrate in the presence of Cy5-FtsK, ATP, and XerCD. We observed $FtsK_C$ translocations toward the surface when the DNA was in an unsynapsed conformation, as judged by the green FIW ($n = 342$; Fig. 4*A* and Fig. S6). In 30% of these events, at least one frame of FRET was apparent between the Cy3B attached to DNA and Cy5-FtsK, suggesting that $FtsK_C$ remained within ~10 nm of the *dif* site for more than approximately the camera frame time (25 ms). Segmenting the translocation events as before, we observed that unsynapsed XerCD-*dif* acts as a roadblock for $FtsK_C$, with the mean FIW after translocation, 181 nm, matching the location of the surface-distal *dif* site (FIW ≈ 183 nm) (Fig. 4*B*). The dwell times for assembly and residence after translocation were fit (Fig. 4*C*), recovering an assembly time of 0.25 ± 0.03 s and a residence time of 0.50 ± 0.02 s. The assembly times were independent of the presence of XerCD as anticipated, but the residence time after translocation decreased fourfold when $FtsK_C$ encountered XerCD bound to unsynapsed *dif* (compared with when it encountered the biotinylated DNA end), suggesting that interactions between XerD and $FtsK_C$ promote $FtsK_C$ dissociation. This decreased residence time gives us confidence that, under these conditions, it reflects interactions with XerCD bound to *dif*. Only a small minority (<0.5%, $n = 1$) of translocations toward unsynapsed XerCD resulted in a reversal by $FtsK_C$, apparent as an increasing red FIW after residence. The lack of reversals in our data contradicts previous observations (32), where $FtsK_C$ reversed translocation direction after meeting XerCD bound to *dif*. The previous observations were made with QD-labeled $FtsK_C$ trimers, where there was the possibility of multiple $FtsK_C$ trimers tethered to the same QD. This multiple tethering could permit loading of a second $FtsK_C$ motor during the residence time of the original motor at XerCD, and may explain

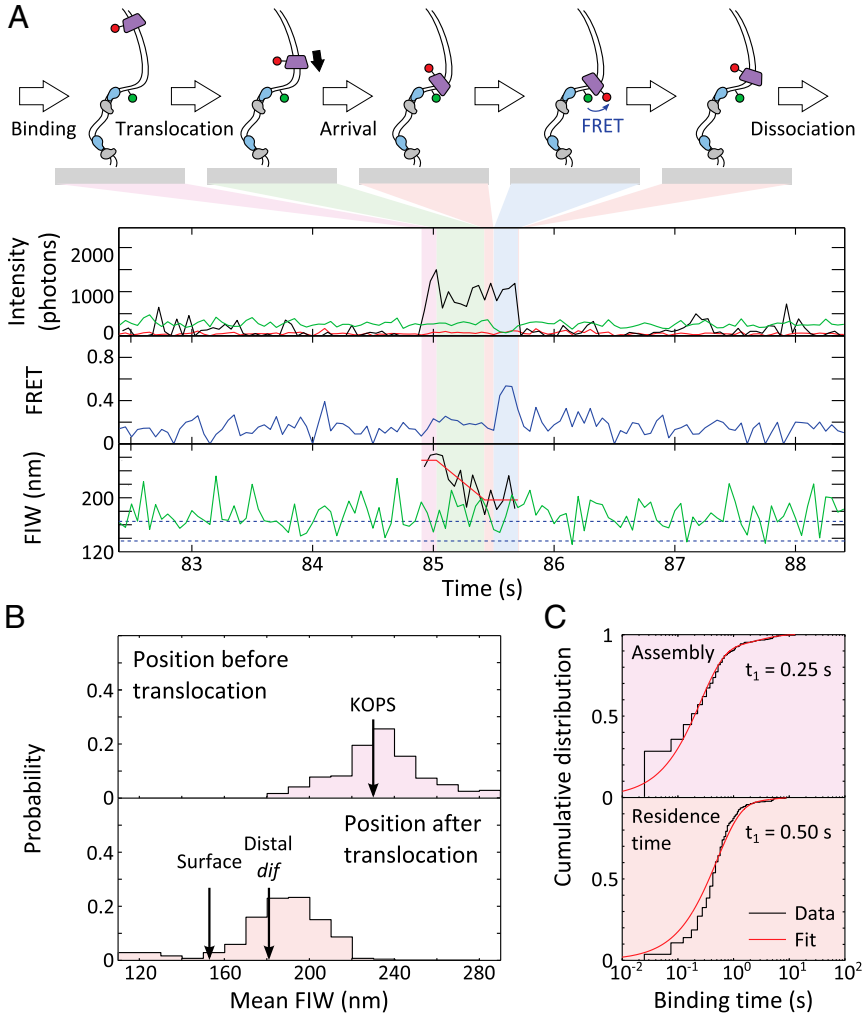

Fig. 4. Translocation stops at unsynapsed XerCD-*dif*. (*A*) Translocation. Blue shading highlights FRET. Translocation towards unsynapsed XerCD-*dif* is apparent in 342 events, of which 102 have at least a single frame of FRET accompanied by anticorrelated *DD* and *DA* changes. (*B*) Start and end positions of translocations. The mean starting FIW is 229 ± 1 nm (±SEM), and the mean end FIW is 181 ± 1 nm (±SEM). (*C*) Dwell times before and after translocation. Distributions are fit in MATLAB (MathWorks) (Table S1).

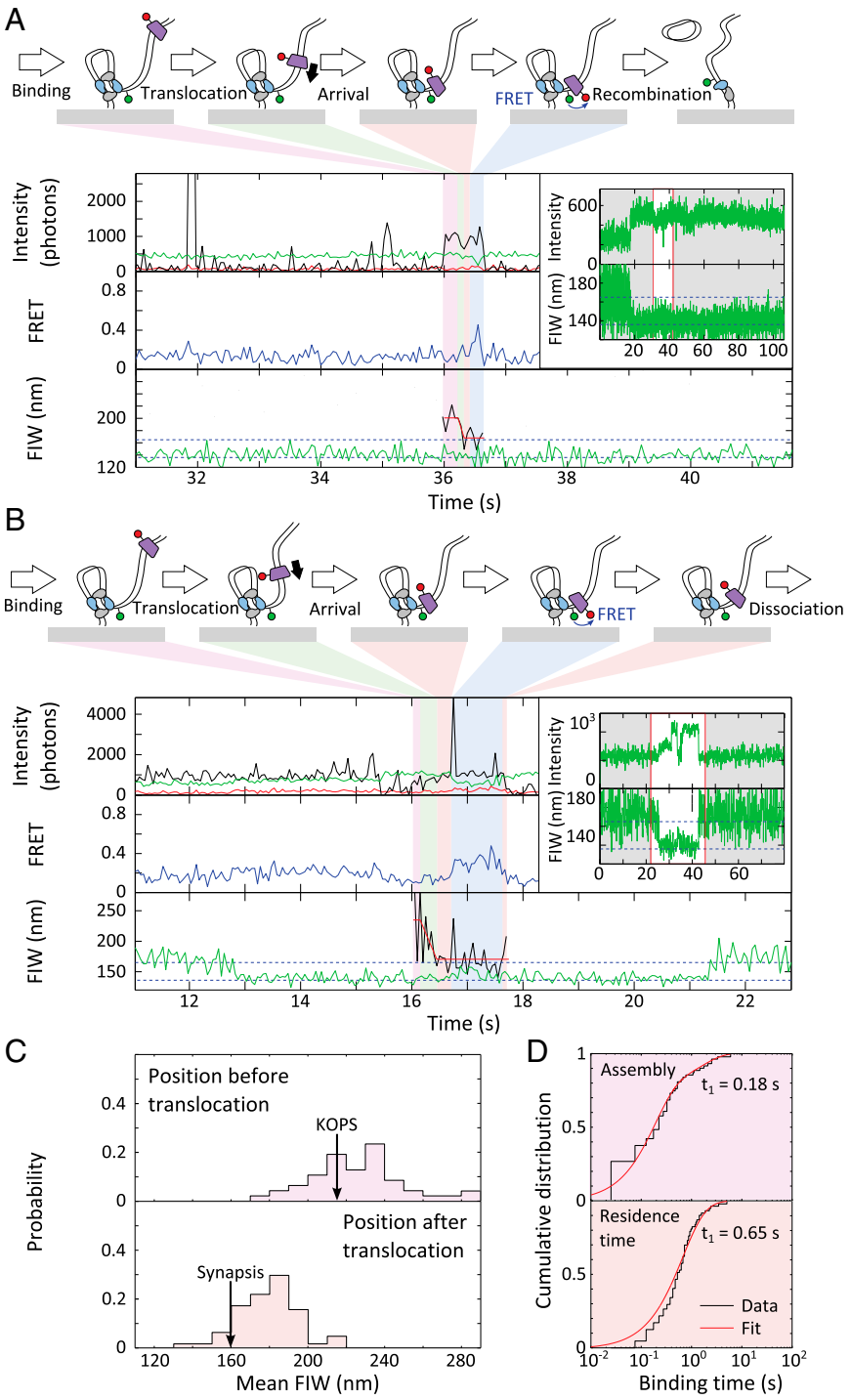

Fig. 5. Arrival of $FtsK_C$ at XerCD-*dif* synapses. (*A*) $FtsK_C$ arrives after synapsis formation, leading to recombination. (*Inset*) Successful recombination reactions result in a permanent narrow green FIW. The highlighted region corresponds to the main figure. $FtsK_C$ binding is apparent after synapsis formation (but not during synapse formation) in 39 of 73 recombination events that meet the 90% confidence criterion. (*B*) $FtsK_C$ arrives at a synapsis and dissociates before the synapsis disassembles. (*Inset*) Synapsis formation and disassembly are apparent as a transiently narrowing FIW ($n = 48$, of which 20 show FRET). (*C*) Start and end positions of translocations. The mean starting FIW is 221 ± 4 nm (±SEM), and the mean end FIW is 175 ± 2 nm (±SEM). (*D*) Dwell times before and after translocation. Distributions are fit using MATLAB (Table S1).

the presence of reversals in the previous observations. The Cy5-FtsK used in this work had only one trimer of $FtsK_C$ per fluorescent label, and hence overcomes this limitation. In the presence of XerCD, we recovered a mean translocation time of 0.18 ± 0.02 s (±SEM), which is shorter than the translocation time (0.33 ± 0.02 s) observed in the absence of XerCD, which, given the shorter translocation distance from the KOPS to XerD, corresponds to a similar mean translocation speed of 15 ± 1 kb·s^{-1}.

$FtsK_C$ activates XerCD recombination at *dif*, which was apparent as DNA molecules that transitioned to a persistent narrow green FIW (Fig. S7*A*). Of these events, 90% that had remained with a narrow FIW for at least 43 s had recombined (rather than being long-lived

synapses; *Methods*), and we define a recombination event as meeting this criterion ($n = 73$). In 50% of recombination events ($n = 39$), $FtsK_C$ binding was apparent after synapsis formation (Fig. 5*A*). In 8% of recombination events ($n = 6$), obvious translocation (consisting of binding followed by a decreasing image width without any anomalous changes in intensity) accompanied recombination (Fig. 5*A*). Obvious translocations did not accompany all recombination events because translocations may not have initiated at the KOPS, and hence would have been too short to resolve in our assays, and because recombination could have been activated by the ~25% of $FtsK_C$ complexes that would carry no fluorescent label. If translocation-induced looping (leading to formation of a synapsis) were a prerequisite for the activation of recombination, it would have been apparent as a $FtsK_C$ presence during synapsis formation. However, only 10% of recombination events ($n = 8$) followed this pattern (Fig. S7*B*), suggesting that translocation-induced looping between *dif* sites was not necessary for the activation of recombination. This suggestion is consistent with the previous result that the formation of the XerCD-*dif* synapsis is independent of $FtsK_C$ (24).

FtsK can resolve catenated chromosomes produced by replication (41). We have previously suggested that FtsK may facilitate this decatenation by remaining in the vicinity of XerCD-*dif* after the activation of recombination and activating multiple rounds of recombination (12, 24). Taking the residence time (during synapsis) of the first $FtsK_C$ to dissociate after the synapsis formation that leads to recombination [i.e., the best candidate for having activated the recombination (Fig. S7*C*)], we recovered a residence time of 0.9 ± 0.2 s. This residence time is the total time from the first observation of binding (or synapsis formation) until $FtsK_C$ dissociates, and is hence an overestimation of the time $FtsK_C$ spends at XerCD-*dif*. Despite this overestimation, it is still shorter than the 1.6 s it takes XerCD to complete the recombination reaction (24), suggesting that $FtsK_C$ does not reside at XerCD long enough to activate multiple further rounds of recombination.

Not all translocations toward synapsed XerCD-*dif* resulted in recombination. We analyzed these nonproductive translocation events, distinguished by a transiently narrowing green FIW (Fig. 5*B* and Fig. S8); of 65 events, around a quarter showed $FtsK_C$ present during synapsis disassembly (Fig. S8). Again, XerCD acted as a roadblock for $FtsK_C$, with the end of translocation approximately matching the position of the synapsis (Fig. 5*C*). FRET was apparent after translocation in 46% of events. For all these translocations toward a synapsis, the assembly time was 0.18 ± 0.4 s, consistent with the assembly time on unsynapsed DNA, and the posttranslocation residence time was 0.65 ± 0.07 s, again consistent with the residence time at unsynapsed XerCD-*dif* (Fig. 5*D*), as well as with the residence time of $FtsK_C$ during productive recombination events (0.9 ± 0.2 s). From this consistency, we infer that $FtsK_C$ does not reside for a significantly longer or shorter time depending on whether it encounters a single XerCD-*dif* or a XerCD-*dif* synaptic complex, or depending on whether it has activated recombination.

FRET may represent a transient association between Cy5-FtsK and XerCD-*dif* complexes. The automatic extraction of FRET events (*Methods*) required a minimum duration of 0.1 s (two frames), and so an upper bound on the duration of this association was estimated (Fig. S9). We find that FRET events had a dwell time of 0.30 ± 0.04 s and 0.23 ± 0.02 s for DNA in the substrate and product configurations, respectively. The dwell after FRET (before dissociation) was 0.09 ± 0.02 s and 0.07 ± 0.01 s for DNA in the substrate and product configurations, respectively. These dwells, between the end of FRET and dissociation, are shorter than the mean translocation time of 0.18 ± 0.02 s, suggesting there is no time for $FtsK_C$ to reverse and translocate after leaving the proximity of XerCD, consistent with the absence of an increasing FIW before dissociation, confirming that $FtsK_C$ dissociates, rather than reverses, after meeting XerCD-*dif*.

Discussion

$FtsK_C$ Translocates on DNA as a Single Hexamer. In this work, using labeled $FtsK_C$ trimers, we addressed the question of whether $FtsK_C$ functions as a single or double hexamer. Double hexamers of $FtsK_C$ have been observed using EM and in crystal structures of $FtsK_C$, and they have been implicated in the explanation of translocation reversals, and the extrusion of DNA loops, in optical tweezers single-molecule experiments (17, 28, 30). Our precise fluorescence measurements unequivocally show that $FtsK_C$ assembles on DNA into a single hexamer, rather than by forming a solution hexamer that then loads onto DNA and subsequently translocates as a single hexamer. Moreover, our data show that $FtsK_C$ activates XerCD-*dif* recombination as a single hexamer. We therefore conclude that double hexamers may not be physiologically relevant. Consistent with our observations, previous biochemical analysis using FtsK monomers led to the proposal that $FtsK_c$ assembles on DNA from monomers in a stepwise fashion (26). These results contrast with the demonstration that *Bacillus subtilis* SpoIIIE, a FtsK ortholog, forms hexamers in the absence of DNA at comparable concentrations to those concentrations used here (42, 43).

As revealed by a structural analysis, three FtsK γ-subdomains bind a KOPS (44). Hence, it seems likely that interaction of a single FtsK trimer with a KOPS will allow the engagement of the three γ-domains with DNA, supporting the physiological relevance of the transient association time, 0.84 ± 0.07 s, that we determined for a single trimer and DNA. The onset of hexamer translocation happens on a similar time scale (~0.25 s; Fig. 6*A*), indicating that assembly of a second trimer into a functional hexamer and subsequent translocation are rapid, and will be dependent on the local concentration of $FtsK_C$ in the cell. A short initial association may serve to prevent $FtsK_C$ from assembling and translocating on DNA when its local concentration is low, which is the case during most of the cell cycle. In vivo, FtsK translocation occurs only when its concentration is high, at an invaginating septum (36, 45).

Previous TPM and optical trapping experiments have required loop extrusion by $FtsK_C$ to observe its action at the single-molecule level. In some of these experiments, large visible $FtsK_C$ aggregates were observed to translocate at the same rate as species observed using loop extrusion in optical trapping (28). It has been suggested that loop extrusion arises from multiple points of contact on the same $FtsK_C$, and that reversals by $FtsK_C$ require that it exists as more than a "single unidirectional motor" (13, 28, 30). Our work establishes that $FtsK_C$ assembles into a single hexamer before translocating, does not usually extrude loops of DNA, and dissociates after it encounters XerCD-*dif*. Hence, we suggest that the loop extrusion and reversals observed in TPM (18) and optical trapping experiments (28, 29) may have been introduced by the surface or by protein aggregates.

$FtsK_C$ Resides Briefly at XerCD-*dif* Before Dissociating. When $FtsK_C$ encountered XerCD bound to *dif*, it resided there with a lifetime of 0.5–1 s, irrespective of whether it encountered an unsynapsed or synapsed XerCD-*dif* complex and independent of whether the encounter led to recombination (Figs. 4–6 *B* and *C*). This pause time is consistent with the pause time observed following collisions of QD-labeled $FtsK_C$ trimers with XerCD-*dif* or XerD-*dif* in studies utilizing DNA curtains (32). However, the outcome of the encounters we observed was different. Although 80% of encounters of QD-labeled $FtsK_C$ with XerCD-*dif* led to reversals of translocation direction, in our experiments, more than 99% of encounters of Cy5-FtsK led to dissociation. A possible explanation is that the Cy3B label, positioned 1 bp away from the surface-distal XerD binding site, influenced the behavior of $FtsK_C$ in our experiments. However, in the absence of XerCD, the

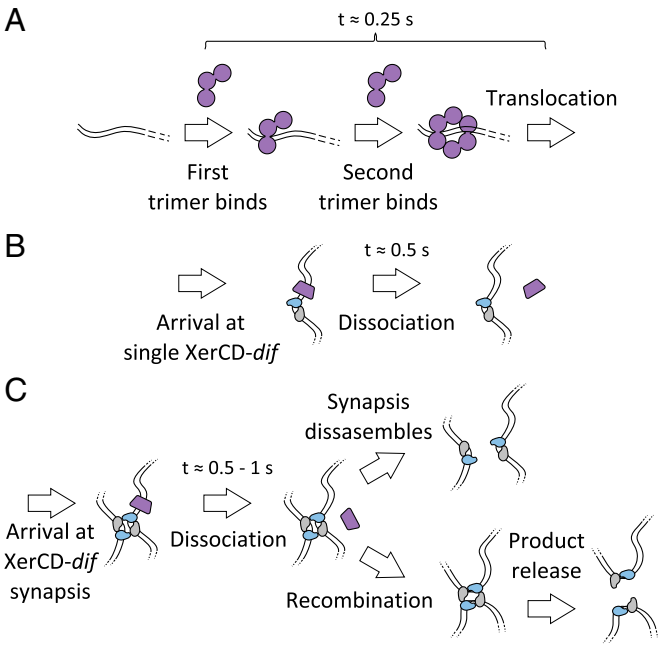

Fig. 6. $FtsK_C$ assembly, stoichiometry, translocation, and activation of recombination. (*A*) $FtsK_C$ assembles stepwise on DNA into a single hexamer, which begins translocating around 0.25 s after the first binding. We note that in vivo $FtsK_C$ is expected to assemble from monomers rather than trimers. (*B*) When $FtsK_C$ arrives at a single *dif* site loaded with XerCD, it resides for around 0.5 s and then dissociates. (*C*) $FtsK_C$ arrives at a preformed XerCD-*dif* synapsis, resides for 0.5–1 s, and then dissociates. Frequently, the synapsis then disassembles, but, occasionally, recombination is activated.

translocation of Cy5-FtsK was not impeded by the Cy3B linkage on DNA, and when Cy5-FtsK encountered another obstruction, the biotin-neutravidin used for surface attachment, we did not observe reversals. We note that in our previous work, the activation of recombination was no less efficient when a fluorophore was placed in the position used here (24). It is also possible that our assay would not be able to resolve a rapid translocation away from XerCD-*dif*; however, using the time between the disappearance of FRET and the disappearance of fluorescence marking the disassociation of Cy5-FtsK, we have established that the average time of 0.08 ± 0.02 s that $FtsK_C$ appeared to remain on DNA after leaving the XerCD-*dif* complex was too short for it to have translocated off the "free end" of our DNA (which would have taken 0.18 ± 0.02 s at the measured translocation velocity). Because we had no more than one trimer of $FtsK_C$ per Cy5 fluorophore in our experiments, we suggest that QD-labeled $FtsK_C$ could have had other $FtsK_C$ trimers, attached to the same fluorescent probe, which might have assembled on DNA during residence at XerD. Because assembly before translocation took ∼0.25 s, and because the residence time at XerCD-*dif* was ∼0.5 s, there is sufficient time for the assembly of a second hexamer, attached to the same QD, while the first resides at XerCD-*dif*.

$FtsK_C$ Activates a Single Round of Recombination Before Dissociating from DNA. Using single-color TFM-FRET, we previously determined that $FtsK_C$ activates recombination by inducing the remodeling of preexisting XerCD-*dif* synapses (24). In these experiments, we deduced the fate of $FtsK_C$ after activation by following the disappearance of PIFE, which resulted from the close proximity of $FtsK_C$ to the recombining complex. The PIFE signal was only observed up to isomerization of the HJ, which was generated by XerD-mediated DNA strand exchanges, which initiate FtsK-dependent recombination. This disappearance of PIFE, however, could not determine $FtsK_C$ dissociation from the complex, because the HJ isomerization could also lead to a change in conformation, which, in turn, could lead to the end of PIFE, because PIFE is only sensitive to distance changes in the range of 1–2 nm (25). Here, using a labeled trimer of $FtsK_C$, we have followed precisely the presence of $FtsK_C$ at the recombining complex. Our results show that $FtsK_C$ predominantly dissociated 0.5–1 s after arriving at XerCD-*dif*. Because HJ formation and resolution by XerCD takes an average of 1.6 s (24), it seems unlikely that FtsK can activate subsequent rounds of recombination without dissociation, rebinding DNA, and encountering the XerCD-*dif* complex de novo. Therefore, multiple rounds of recombination would have to be mediated by multiple arrivals of $FtsK_C$ hexamers at XerCD-*dif*. The rapid dissociation of $FtsK_C$, observed once it encounters XerCD-*dif*, may prevent a $FtsK_C$ hexamer from blocking access to XerCD-*dif* during these subsequent activation attempts by other $FtsK_C$ hexamers.

The vast majority of the events where FtsK successfully activated XerCD-*dif* recombination were not accompanied by any evidence of translocation-mediated looping. This lack of looping provides more evidence to support the conclusion that FtsK remodels existing initial synapses (24), rather than extruding a loop and forming an active synapsis or otherwise promoting active synapse assembly as suggested by TPM experiments using a purified γ-subdomain (13, 46, 47).

Most frequently, when $FtsK_C$ encountered a XerCD-*dif* synapsis, recombination was not activated. If FtsK behaves in a similar fashion in vivo, this low likelihood of activation would serve as a regulatory mechanism to help ensure it resolves, rather than produces, chromosome dimers. Only when a synapsis reformed several times, because chromosome topology was preventing segregation, would recombination, on average, be activated.

Two-Color TFM-FRET Follows Two Effective Lengths Along the Same DNA. The extension of TFM, using two spectrally distinct fluorophores to track two positions simultaneously along the same DNA, has allowed us to correlate large-scale DNA conformation with the behavior of $FtsK_C$ as it assembled, translocated, and interacted with XerCD-*dif*. This method, performed on a standard fluorescence microscope, provides a blueprint for single-molecule experiments with increasing bandwidth, allowing the study of increasingly complicated protein–nucleic acid systems. This work has encoded information in the intensities, widths, and positions of the images of two fluorophores, realizing the possibility of six simultaneous fluorescence observables (increased further with the use of ALEX). TFM-FRET can be extended with the introduction of a third spectral channel (3, 48) and a third excitation laser, which would allow up to three simultaneous FRET distances, colocalization of three binding partners, and the simultaneous measurement of three distances along the same DNA molecule.

Methods

Standard methods were used for DNA and protein preparation, and they are described in detail in *SI Text*. Sample preparation and single-molecule experiments are described in *SI Text*. Data analysis, including event extraction, dwell time fitting, and the segmentation of translocation, is described in *SI Text*. The procedure for correcting Cy5 intensity and predicting the intensity distribution of labeled FtsK is described in *SI Text*.

ACKNOWLEDGMENTS. P.F.J.M. was supported by MathWorks (Cambridge, UK). P.Z. was supported by the Leverhulme Trust (Grant RP2013-K-017). Work in the D.J.S. laboratory was supported by a Wellcome Trust Senior Investigator Award (Grant 099204/Z/12Z). Work in the A.N.K. laboratory was supported by the European Commission Seventh Framework Program (Grant FP7/2007-2013 HEALTH-F4-2008-201418), the Biotechnology and Biological Research Council (Grant BB/H01795X/1), and the European Research Council (Starter Grant 261227).

1. Hohng S, et al. (2007) Fluorescence-force spectroscopy maps two-dimensional reaction landscape of the holliday junction. *Science* 318(5848):279–283.
2. Harms GS, et al. (2003) Probing conformational changes of gramicidin ion channels by single-molecule patch-clamp fluorescence microscopy. *Biophys J* 85(3):1826–1838.
3. Lee S, Lee J, Hohng S (2010) Single-molecule three-color FRET with both negligible spectral overlap and long observation time. *PLoS One* 5(8):e12270.
4. Lee J, et al. (2010) Single-molecule four-color FRET. *Angew Chem Int Ed Engl* 49(51):9922–9925.
5. Bigot S, Sivanathan V, Possoz C, Barre F-X, Cornet F (2007) FtsK, a literate chromosome segregation machine. *Mol Microbiol* 64(6):1434–1441.
6. Barre F-X (2007) FtsK and SpoIIIE: The tale of the conserved tails. *Mol Microbiol* 66(5):1051–1055.
7. Kaimer C, Graumann PL (2011) Players between the worlds: Multifunctional DNA translocases. *Curr Opin Microbiol* 14(6):719–725.
8. Stouf M, Meile J-C, Cornet F (2013) FtsK actively segregates sister chromosomes in Escherichia coli. *Proc Natl Acad Sci USA* 110(27):11157–11162.
9. Aussel L, et al. (2002) FtsK Is a DNA motor protein that activates chromosome dimer resolution by switching the catalytic state of the XerC and XerD recombinases. *Cell* 108(2):195–205.
10. Hallet B, Sherratt DJ (1997) Transposition and site-specific recombination: Adapting DNA cut-and-paste mechanisms to a variety of genetic rearrangements. *FEMS Microbiol Rev* 21(2):157–178.
11. Sherratt DJ, et al. (1995) Site-specific recombination and circular chromosome segregation. *Philos Trans R Soc Lond B Biol Sci* 347(1319):37–42.
12. Grainge I, et al. (2007) Unlinking chromosome catenanes in vivo by site-specific recombination. *EMBO J* 26(19):4228–4238.
13. Ip SCY, Bregu M, Barre FX, Sherratt DJ (2003) Decatenation of DNA circles by FtsK-dependent Xer site-specific recombination. *EMBO J* 22(23):6399–6407.
14. Barre F-X, Sherratt DJ (2005) Chromosome dimer resolution. *The Bacterial Chromosome*, ed Higgins NP (American Society for Microbiology, Washington, DC), pp 513–524.
15. Draper GC, McLennan N, Begg K, Masters M, Donachie WD (1998) Only the N-terminal domain of FtsK functions in cell division. *J Bacteriol* 180(17):4621–4627.
16. Yu XC, Weihe EK, Margolin W (1998) Role of the C terminus of FtsK in Escherichia coli chromosome segregation. *J Bacteriol* 180(23):6424–6428.
17. Massey TH, Mercogliano CP, Yates J, Sherratt DJ, Löwe J (2006) Double-stranded DNA translocation: Structure and mechanism of hexameric FtsK. *Mol Cell* 23(4):457–469.
18. Ptacin JL, Nöllmann M, Bustamante C, Cozzarelli NR (2006) Identification of the FtsK sequence-recognition domain. *Nat Struct Mol Biol* 13(11):1023–1025.
19. Bigot S, et al. (2005) KOPS: DNA motifs that control E. coli chromosome segregation by orienting the FtsK translocase. *EMBO J* 24(21):3770–3780.
20. Sivanathan V, et al. (2006) The FtsK gamma domain directs oriented DNA translocation by interacting with KOPS. *Nat Struct Mol Biol* 13(11):965–972.
21. Bigot S, Corre J, Louarn J-M, Cornet F, Barre F-X (2004) FtsK activities in Xer recombination, DNA mobilization and cell division involve overlapping and separate domains of the protein. *Mol Microbiol* 54(4):876–886.
22. Massey TH, Aussel L, Barre F-X, Sherratt DJ (2004) Asymmetric activation of Xer site-specific recombination by FtsK. *EMBO Rep* 5(4):399–404.
23. Yates J, et al. (2006) Dissection of a functional interaction between the DNA translocase, FtsK, and the XerD recombinase. *Mol Microbiol* 59(6):1754–1766.
24. Zawadzki P, et al. (2013) Conformational transitions during FtsK translocase activation of individual XerCD-dif recombination complexes. *Proc Natl Acad Sci USA* 110(43):17302–17307.
25. Hwang H, Kim H, Myong S (2011) Protein induced fluorescence enhancement as a single molecule assay with short distance sensitivity. *Proc Natl Acad Sci USA* 108(18):7414–7418.
26. Graham JE, Sherratt DJ, Szczelkun MD (2010) Sequence-specific assembly of FtsK hexamers establishes directional translocation on DNA. *Proc Natl Acad Sci USA* 107(47):20263–20268.
27. Graham JE, Sivanathan V, Sherratt DJ, Arciszewska LK (2010) FtsK translocation on DNA stops at XerCD-dif. *Nucleic Acids Res* 38(1):72–81.
28. Pease PJ, et al. (2005) Sequence-directed DNA translocation by purified FtsK. *Science* 307(5709):586–590.
29. Levy O, et al. (2005) Identification of oligonucleotide sequences that direct the movement of the Escherichia coli FtsK translocase. *Proc Natl Acad Sci USA* 102(49):17618–17623.
30. Saleh OA, Pérals C, Barre FX, Allemand JF (2004) Fast, DNA-sequence independent translocation by FtsK in a single-molecule experiment. *EMBO J* 23(12):2430–2439.
31. Lee JY, Finkelstein IJ, Crozat E, Sherratt DJ, Greene EC (2012) Single-molecule imaging of DNA curtains reveals mechanisms of KOPS sequence targeting by the DNA translocase FtsK. *Proc Natl Acad Sci USA* 109(17):6531–6536.
32. Lee JY, Finkelstein IJ, Arciszewska LK, Sherratt DJ, Greene EC (2014) Single-molecule imaging of FtsK translocation reveals mechanistic features of protein-protein collisions on DNA. *Mol Cell* 54(5):832–843.
33. Pinkney JNM, et al. (2012) Capturing reaction paths and intermediates in Cre-loxP recombination using single-molecule fluorescence. *Proc Natl Acad Sci USA* 109(51):20871–20876.
34. May PFJ, et al. (2014) Tethered fluorophore motion: Studying large DNA conformational changes by single-fluorophore imaging. *Biophys J* 107(5):1205–1216.
35. Crozat E, et al. (2010) Separating speed and ability to displace roadblocks during DNA translocation by FtsK. *EMBO J* 29(8):1423–1433.
36. Bisicchia P, Steel B, Mariam Debela MH, Löwe J, Sherratt D (2013) The N-terminal membrane-spanning domain of the Escherichia coli DNA translocase FtsK hexamerizes at midcell. *MBio* 4(6):e00800–e00813.
37. Kapanidis AN, et al. (2004) Fluorescence-aided molecule sorting: Analysis of structure and interactions by alternating-laser excitation of single molecules. *Proc Natl Acad Sci USA* 101(24):8936–8941.
38. Chivers CE, et al. (2010) A streptavidin variant with slower biotin dissociation and increased mechanostability. *Nat Methods* 7(5):391–393.
39. Kass RE, Raftery AE (1995) Bayes factors. *J Am Stat Assoc* 90(420):773–795.
40. Periz J, et al. (2013) Rotavirus mRNAS are released by transcript-specific channels in the double-layered viral capsid. *Proc Natl Acad Sci USA* 110(29):12042–12047.
41. Shimokawa K, Ishihara K, Grainge I, Sherratt DJ, Vazquez M (2013) FtsK-dependent XerCD-dif recombination unlinks replication catenanes in a stepwise manner. *Proc Natl Acad Sci USA* 110(52):20906–20911.
42. Cattoni DI, et al. (2014) Structure and DNA-binding properties of the Bacillus subtilis SpoIIIE DNA translocase revealed by single-molecule and electron microscopies. *Nucleic Acids Res* 42(4):2624–2636.
43. Cattoni DI, et al. (2013) SpoIIIE mechanism of directional translocation involves target search coupled to sequence-dependent motor stimulation. *EMBO Rep* 14(5):473–479.
44. Löwe J, et al. (2008) Molecular mechanism of sequence-directed DNA loading and translocation by FtsK. *Mol Cell* 31(4):498–509.
45. Hale CA, de Boer PAJ (2002) ZipA is required for recruitment of FtsK, FtsQ, FtsL, and FtsN to the septal ring in Escherichia coli. *J Bacteriol* 184(9):2552–2556.
46. Diagne CT, et al. (2014) TPM analyses reveal that FtsK contributes both to the assembly and the activation of the XerCD-dif recombination synapse. *Nucleic Acids Res* 42(3):1721–1732.
47. Besprozvannaya M, Burton BM (2014) Do the same traffic rules apply? Directional chromosome segregation by SpoIIIE and FtsK. *Mol Microbiol* 93(4):599–608.
48. Hohng S, Joo C, Ha T (2004) Single-molecule three-color FRET. *Biophys J* 87(2):1328–1337.
49. Kapanidis AN (2008) Alternating-laser excitation of single molecules. *Single-Molecule Techniques: A Laboratory Manual*, eds Selvin PR, Ha T (Cold Spring Harbor Laboratory Press, Plainview, NY), pp 85–119.
50. Ferreira H, Sherratt D, Arciszewska L (2001) Switching catalytic activity in the XerCD site-specific recombination machine. *J Mol Biol* 312(1):45–57.
51. Gasteiger E, et al. (2005) Protein identification and analysis tools on the ExPASY server. *The Proteomics Protocols Handbook*, ed Walker JM (Humana Press, Totowa, NJ), pp 571–607.
52. Holden SJ, et al. (2010) Defining the limits of single-molecule FRET resolution in TIRF microscopy. *Biophys J* 99(9):3102–3111.
53. Evans GW, Hohlbein J, Craggs T, Aigrain L, Kapanidis AN (2015) Real-time single-molecule studies of the motions of DNA polymerase fingers illuminate DNA synthesis mechanisms. *Nucleic Acids Res* 43(12):5998–6008.